Fermi National Accelerator Laboratory

FERMILAB-Conf-75/67-THY
August 1975

For Proceedings of the International Conference on High Energy Physics, Palermo, Italy, 23-28 June 1975.

WHAT ARE TOTAL CROSS SECTION DATA TRYING TO TELL US?

Harry J. Lipkin*)

Weizmann Institute of Science, Rehovot, Israel
Argonne National Laboratory, Argonne, Illinois 60439 and
Fermi National Accelerator Laboratory, Batavia, Illinois 60510

Hadron-nucleon total cross sections have been observed experimentally to decrease at low energies and go through a minimum and start rising at higher energies[1]. In plots of total cross sections as a function of energy the curves for different processes appear to be very different from one another. But there are striking regularities in the data[2] which become apparent when they are plotted somewhat differently.

There is no physical basis for the standard plot shown in Fig. 1 of σ_{total} vs. laboratory momentum with a logarithmic scale for P_{lab}. Why not plot instead the imaginary part of the forward scattering amplitude against center-of-mass momentum? At high energies this is equivalent to the plot in Fig. 2 of $\sigma_{total} \times \sqrt{P_{lab}/2Q}$ against $\sqrt{P_{lab}}$. Although the same data are plotted in both figures, Fig. 1 shows very different curves for the six different processes while Fig. 2 shows six slightly curved lines which look very similar to one another. The K^+p and K^-p lines are very nearly parallel and similarly for π^+p and π^-p and $\bar{p}p$ and pp. Figure 3 shows the same plots on an expanded scale. The $\bar{p}p$ and pp cross sections are multiplied by the scaling factor 2/3 given by the quark model, and the scale in Fig. 3b is expanded by subtracting the constant 23 mb from all cross sections.

The real phenomenological motivation for the plots of Figs. 2 and 3 comes from the two-component description[3] of total cross sections as the sum of a Regge component which decreases roughly like $s^{-1/2}$ and a Pomeron component which varies slowly with energy.

$$\sigma_{tot}(s) = R \cdot s^{-1/2} + f(s) \tag{1}$$

where R is the strength of the Regge component for the particular process and f(s) is a slowly varying function which may be different for different processes. Let us define

$$x \equiv s^{1/2} \tag{2a}$$

$$y \equiv s^{1/2}\sigma_{tot}(s) = R + x f(x^2). \tag{2b}$$

Since P_{lab} is proportional to s at high energies the quantities defined by Eqs. (2) are just the abscissa and ordinate of Fig. 2.

Comparison of Eqs. (1) and (2b) clarifies the contrast between the complexity of the plots of Fig. 1 described by Eq. (1) and the simplicity of the plots of Fig. 2 described

*)Supported in part by the Israel Commission for Basic Research and the U. S. Energy Research and Development Administration.

by Eq. (2b). The right-hand side of Eq. (1) contains two terms. The Regge term decreases with energy while the Pomeron is either constant or decreases slowly at low energies and rises at higher energies. The coefficient R of the decreasing Regge term differs widely between different processes. It is very large in $\sigma(\bar{p}p)$ which decreases monotonically up to $P_{lab} = 200$ GeV/c, but very small for $\sigma(K^+p)$ which begins to rise at a very low energy. The large differences in the curves of total cross section versus energy arise because the Regge term responsible for the most rapid energy variation has very different values for different processes.

In the representation of the data by Fig. 2 and Eq. (2b) the Regge contribution appears as a constant. Pairs of curves for particle and antiparticle scattering which differ only in their Regge contribution appear vertically displaced from one another with very little change in shape, in contrast to the plots of Fig. 1 where differences in the Regge contribution give curves having very different shapes. The simplicity of the plots of Figs. 2 and 3 confirm that $s^{-1/2}$ gives a very good description of the energy dependence of the Regge contribution. The relative magnitudes of the splittings agree with predictions from the conventional Regge description with duality or exchange degeneracy[4]. The splitting between the two kaon-nucleon curves is larger than the pion-nucleon splitting and smaller than the nucleon-nucleon splitting.

The manner in which the pion-nucleon curves lie between the kaon-nucleon and nucleon-nucleon curves is very surprising and is a manifestation of a phenomenological regularity observed in the Pomeron component of the total cross section[5]

$$P(\pi p) = (1/2)P(Kp) + (1/3)P(pp) \tag{3}$$

where P denotes the Pomeron contribution. This is seen in Fig. 3 in which the following two linear combinations of $\sigma(KN)$ and $\sigma(NN)$ having the form of the right-hand side of Eq. (3) are also plotted.

$$\sigma_A = (1/2)\sigma(K^+p) + (1/2)\sigma(pp) \tag{4a}$$

$$\sigma_B = (1/2)\sigma(K^+p) + (1/3)\sigma(\bar{p}p). \tag{4b}$$

These are seen to have the same qualitative behavior as $\sigma(\pi N)$ and very different from $\sigma(NN)$ and $\sigma(KN)$, while displaced from $\sigma(\pi N)$ by constant amounts consistent with their Regge description.

What are these curves trying to tell us? Figures 2 and 3 demonstrate the validity of the two component description (1). But our level of understanding of the two components is very different. The Regge contribution is reasonably well described by a universal $s^{-1/2}$ energy behavior for all processes and a coefficient R whose relative values are given by exchange degeneracy and duality. The Pomeron component has an energy dependence f(s) which is neither understood nor established, and both its magnitude and energy dependence differ for pions, kaons and nucleons in a manner which is

not understood. The plots of Fig. 1 are dominated by the well-understood Regge component. The plots of Figs. 2 and 3 suppress the Regge component and display the features of the more interesting and less understood Pomeron. If we are interested in what the data are trying to tell us about the Pomeron, Figs. 2 and 3 are better places to look.

Another way to look for regularities in the Pomeron component is to plot linear combinations of the different total cross sections which contain only the Pomeron contribution. The following combinations are constructed to cancel the contributions from the leading Regge trajectories under the assumption of exchange degeneracy.

$$\sigma(\phi N) = \sigma(K^- p) + \sigma(K^+ p) - \sigma(\pi^- p) \tag{5a}$$

$$\Delta(\pi K) = \sigma(\pi^- p) - \sigma(K^- p) \tag{5b}$$

$$\sigma_1(pK) = \frac{3}{2}\sigma(K^+ p) - \frac{1}{3}\sigma(pp) \tag{5c}$$

$$\Delta(MB) = \frac{1}{3}\sigma(pp) - \frac{1}{2}\sigma(Kp) \tag{5d}$$

The quantity $\sigma(\phi N)$, Eq. (5a), is the quark model expression for the ϕ-nucleon cross section; i.e., the scattering of a strange quark-antiquark pair on a proton.

Figure 4 shows plots of these four quantities. They all show very simple energy behavior, and a striking and unexplained equality related to the equality (3) is observed between the curves (5a) and (5c) and the curves (5b) and (5d). These suggest that the Pomeron contains two components, one rising slowly with energy, and the other decreasing slowly. The rising component is seen in $\sigma(\phi N)$, the decreasing component is seen in $\Delta(\pi K)$ and accounts for the difference between $\sigma(\pi N)$ and $\sigma(KN)$. The $K^+ p$ and pp channels are both exotic and have no Regge contributions, but $\sigma(pp)$ and $\sigma(K^+ p)$ have different energy behavior, as indicated in Fig. 1. The linear combinations (5c) and (5d) seem to project out the same two components found in the meson-baryon cross sections $\sigma(\phi N)$ and $\Delta(\pi K)$.

The quantity $\Delta(MB)$ defined by Eq. (5d) should vanish in the additive quark model and represents the difference between the scattering of a "baryonic quark" and a "mesonic quark." The quantity $\Delta(\pi K)$ represents the difference between the scattering of a nonstrange quark and a strange quark. Why these two differences should be equal, as indicated by Fig. 4 is a puzzle which remains to be explained.

REFERENCES

1) A. N. Diddens, in Proc. XVII Intern. Conf. on High Energy Physics, London (1974), ed. J. R. Smith, p. I-41.

2) E. Flaminio, J. D. Hansen, D. R. O. Morrison and N. Tovey, Compilation of Cross Sections. I. Proton Induced Reactions. II. Antiproton Induced Reactions, CERN/HERA 70-2 and 70-3;
E. Bracci, J. P. Droulez, E. Flaminio, J. D. Hansen and D. R. O. Morrison, Compilation of Cross Sections. I. π^- and π^+ Induced Reactions. II. K^- and K^+ Induced Reactions, CERN/HERA 72-1 and 72-3;
J. B. Allaby, Yu. B. Bushnin, Yu. P. Gorin et al., Yad. Fiz. 12, 538 (1970); Phys. Lett. 30B, 500 (1969);
Yu. P. Gorin, S. P. Denisov, S. V. Donskov et al., Yad. Fiz. k4 (1971); Phys. Lett. 36B, 415 (1971);
S. P. Denisov, S. V. Donskov, Yu. P. Gorin et al., Nucl. Phys. B65, 1 (1973);
A. S. Carroll et al., Phys. Rev. Lett. 33, 927, 932 (1974) and FERMILAB-Pub-75151-EXP.

3) H. J. Lipkin, Phys. Rev. Lett. 16, 1015 (1966);
H. J. Lipkin, Z. Phys. 202, 414 (1967).

4) M. Kugler, Acta Phys. Austriaca Suppl. VII, 443 (1970) and references therein;
H. J. Lipkin, Nucl. Phys. B9, 349 (1969);
H. Harari, Phys. Rev. Lett. 22, 562 (1969);
J. L. Rosner, Phys. Rev. Lett. 22, 689 (1969).

5) H. J. Lipkin, Phys. Lett. 56B, 76 (1975);
Phys. Rev. D11, 1827 (1975).

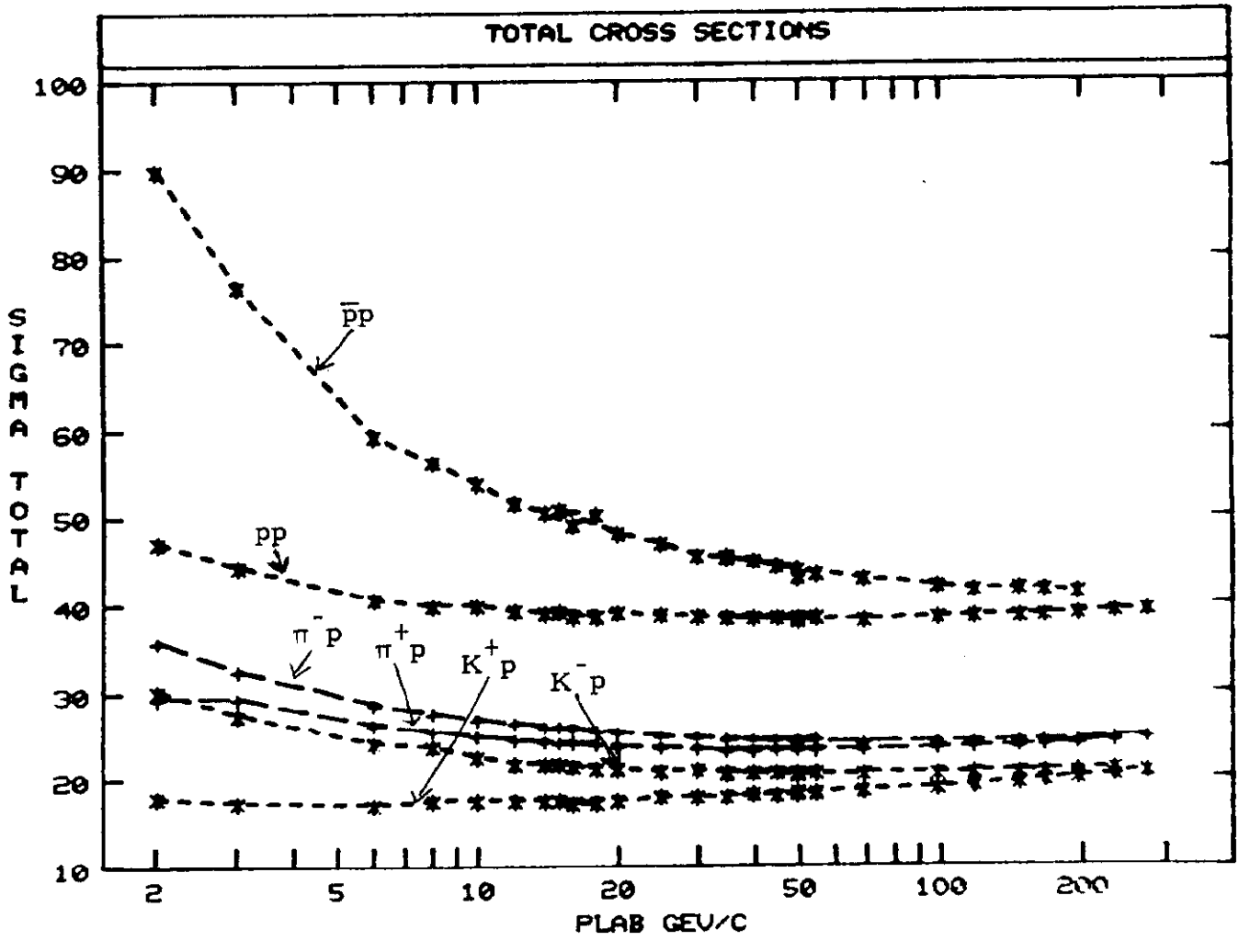

Fig. 1. Total Cross Sections vs. P_{lab}.

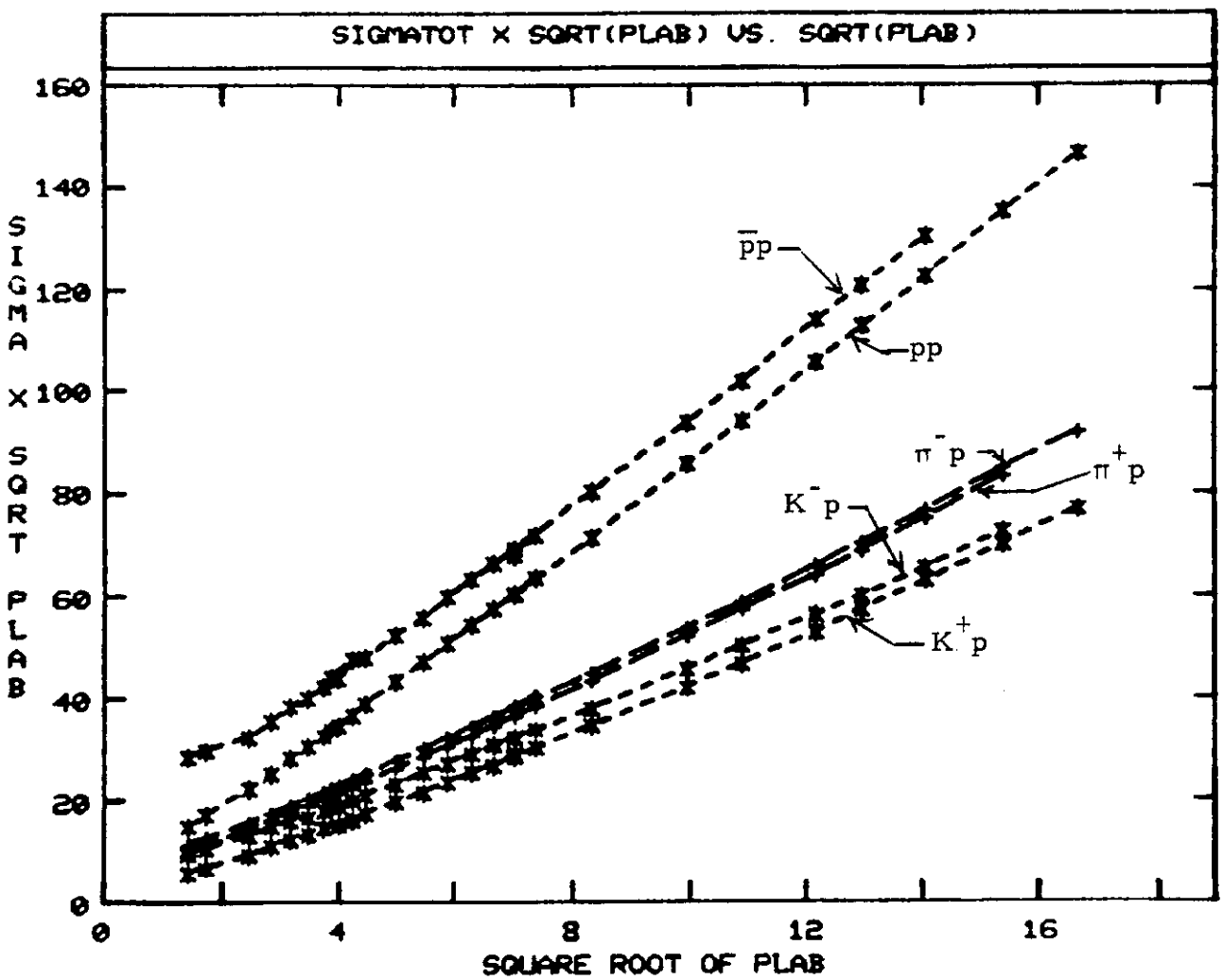

Fig. 2. $\sigma_{tot}\sqrt{P/20}$ vs. $\sqrt{P}$.

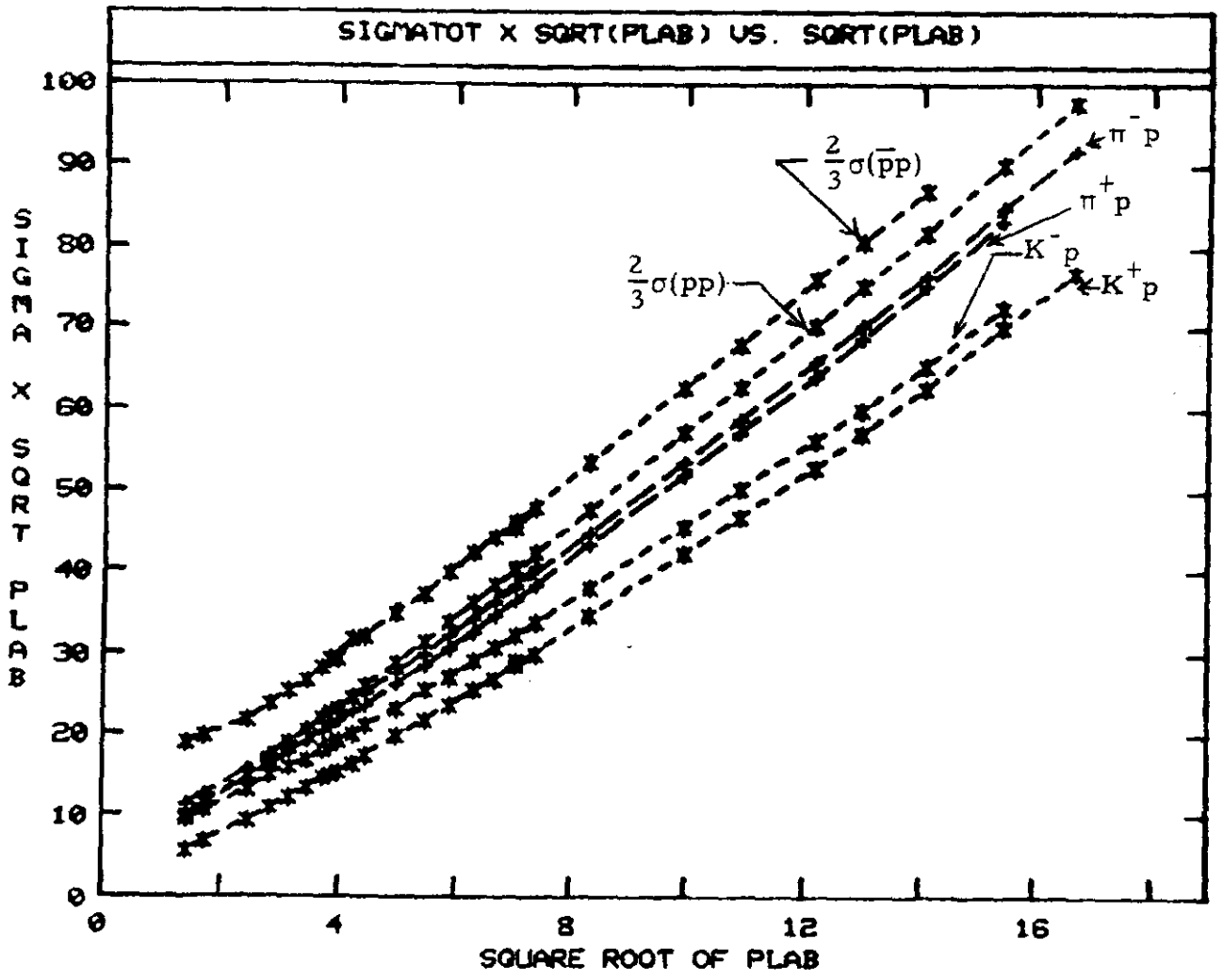

Fig. 3a. $\sigma_{tot}\sqrt{P\ 20}$ vs. $\sqrt{P}$.

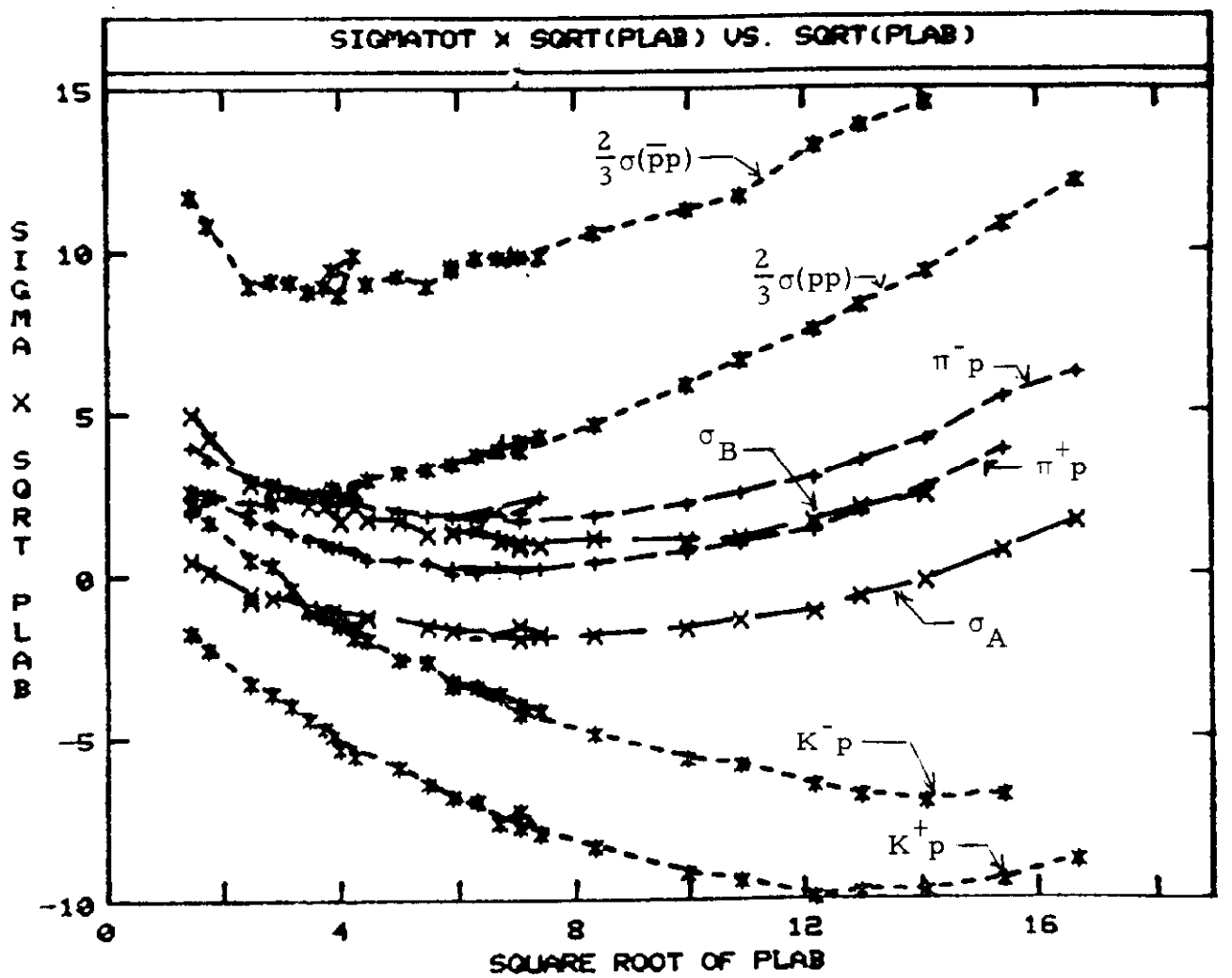

Fig. 3b. $(\sigma-23)\sqrt{P/20}$ vs. $\sqrt{P}$.

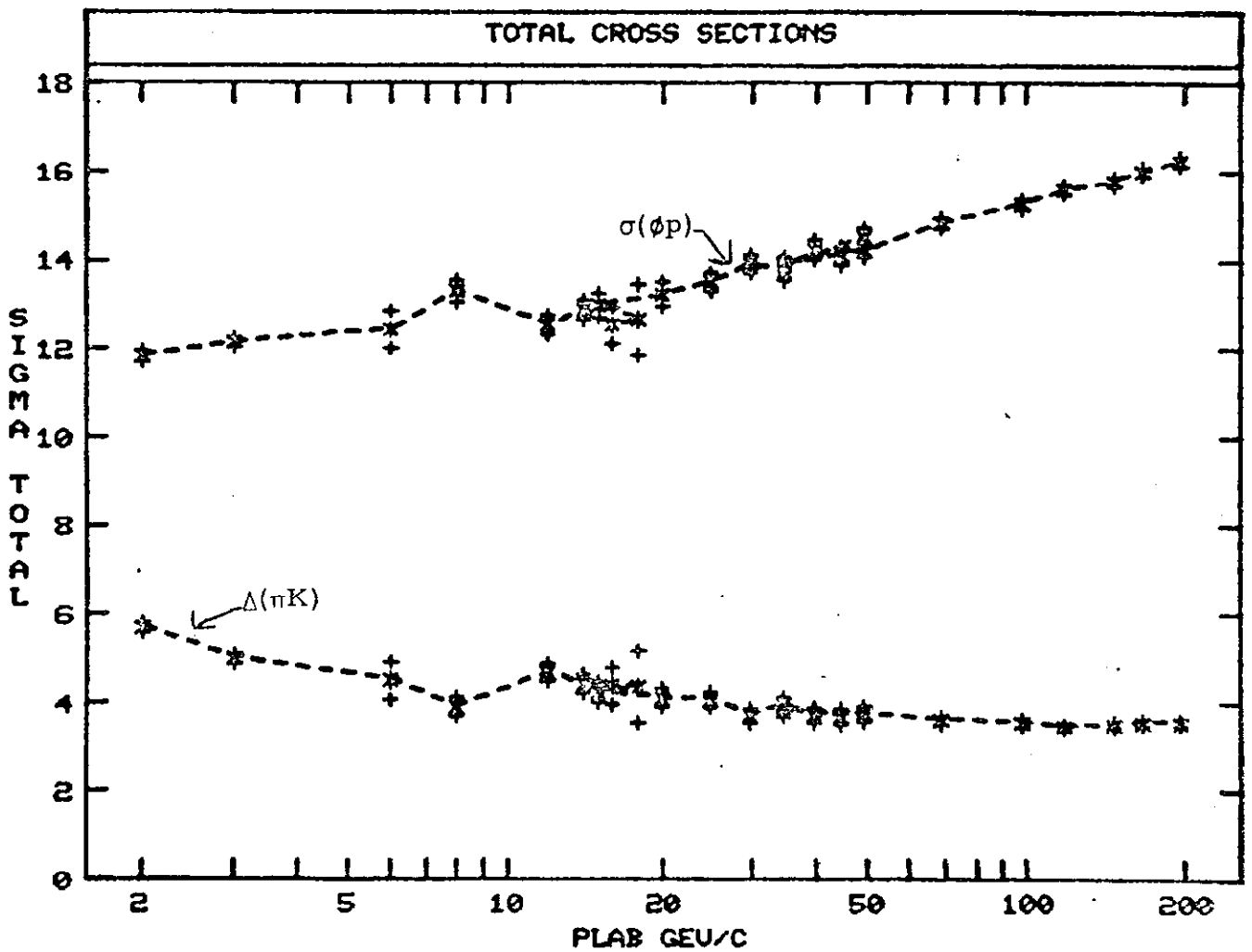

Fig. 4a. $\Delta(\pi K)$ and $\sigma(\phi p)$ vs. P_{lab}.

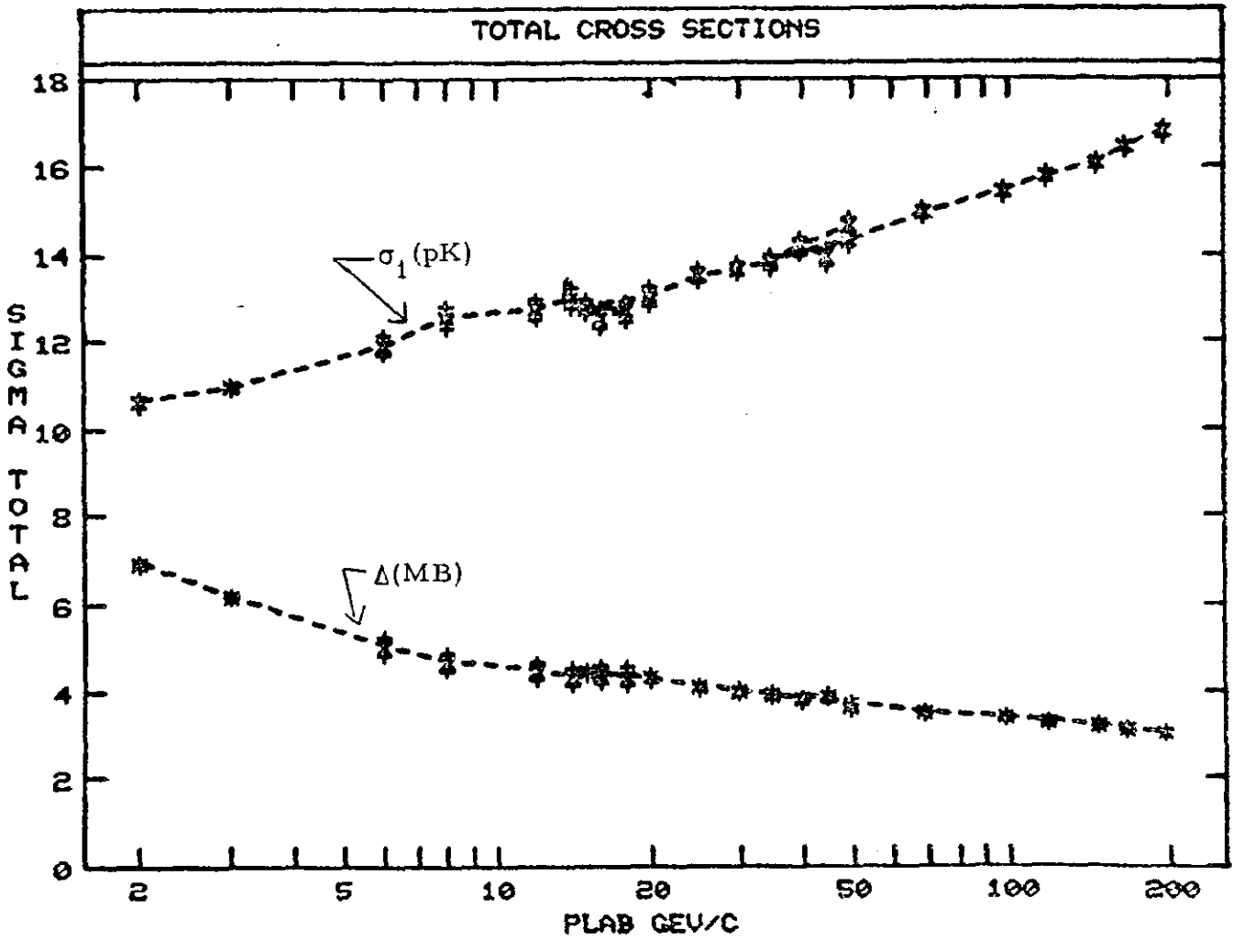

Fig. 4b. Δ(MB) and σ_1(pK) vs. P_{lab}.